Precise Distance Measurement with IEEE 802.15.4 (ZigBee) Devices

Stefan Schwarzer*†, Martin Vossiek†, Markus Pichler‡ and Andreas Stelzer§
*Siemens AG, Otto-Hahn-Ring 6, 81379 Munich, Germany
E-mail: stefan.schwarzer.ext@siemens.com, Phone: ++49 (89) 636 45489, Fax: ++49 (89) 636 43702
†Institute of Electrical Information Technology, Clausthal University of Technology, Germany
‡Linz Center of Mechatronics GmbH, Linz, Austria
§Institute for Communications and Information Engineering, Johannes Kepler University, Linz, Austria

***Abstract*—In modern wireless communications products it is required to incorporate more and more different functions to comply with current market trends. A very attractive function with steadily growing market penetration is local positioning. To add this feature to low-cost mass-market devices without additional power consumption, it is desirable to use commercial communication chips and standards for localization of the wireless units. In this paper we present a concept to measure the distance between two IEEE 802.15.4 (ZigBee) compliant devices. The presented prototype hardware consists of a low-cost $2.45\,\mathrm{GHz}$ ZigBee chipset. For localization we use standard communication packets as transmit signals. Thus simultaneous data transmission and transponder localization is feasible. To achieve high positioning accuracy even in multipath environments, a coherent synthesis of measurements in multiple channels and a special signal phase evaluation concept is applied. With this technique the full available ISM bandwidth of $80\,\mathrm{MHz}$ is utilized. In first measurements with two different frequency references—a low-cost oscillator and a temperatur-compensated crystal oscillator—a positioning bias error of below $16\,\mathrm{cm}$ and $9\,\mathrm{cm}$ was obtained. The standard deviation was less than $3\,\mathrm{cm}$ and $1\,\mathrm{cm}$, respectively. It is demonstrated that compared to signal correlation in time, the phase processing technique yields an accuracy improvement of roughly an order of magnitude.**

I. Introduction

Over the last years several communications standards for wireless sensors have been developed that can establish data links with low data rate and low power consumption for the communication between sensors and infrastructure. Examples are IEEE 802.15.4 (the PHY and MAC layers of ZigBee), Z-Wave or Bluetooth. In the future, communication between sensors will lead to self organizing sensor networks [1]. One important issue will be the possibility of the communicating partners to localize themselves inside the network. Several approaches with ZigBee compliant devices have been presented. Some rely on measurements of the electromagnetic field strength at the reception sites [2], other on the determination of the roundtrip-time-of-flight (RTOF) of the communication signals [3]. The disadvantage of these solutions is either their low localization accuracy or their proprietary design that is not optimized for low power consumption. In order to make localization attractive for sensor networks, it should not considerably stress battery lifetime. An increased robustness against multipath and non-line-of-sight (NLOS) situations is preferable, as sensors are often mounted in locations that are secluded and difficult to access.

In this paper we present results of distance measurements between sensor network nodes compliant to IEEE 802.15.4. The principle is based on a combination of signal time-of-flight and phase measurements. This combination leads to higher measurement accuracy than using just one of the mentioned methods alone. As the ZigBee transmitter hardware remains unchanged, the power consumption is as low as in normal ZigBee communication modes. The demonstrator operates in the $2.45\,\mathrm{GHz}$ ISM (Industrial, Scientific, Medical) band, which is divided into 16 channels spaced $f_d = 5\,\mathrm{MHz}$. The 3dB bandwidth of the signals is approximately $2\,\mathrm{MHz}$. Adoption to other communications standards should be possible in many cases.

II. Measurement setup

A. System setup

Our distance measurement setup uses the time-difference-of-arrival (TDOA) principle for locating a transponder T_1 with unknown position. For one dimensional (1D) distance measurements the setup is shown in Fig. 1. The transmitters T_1 and T_2 are located on a straight line between two receivers R_1 and R_2. If only the position of T_1 is unknown, the quantity to be measured is the distance d_0 between the two transmitters. A generalization to 2D or 3D positioning is possible using additional receivers [4], [5].

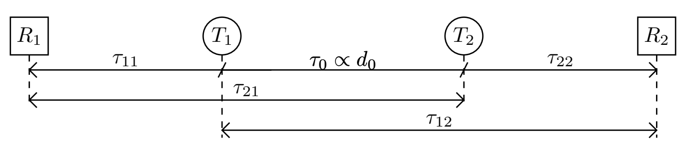

Fig. 1. TDOA setup for 1D distance measurement consisting of two transmitters T_1 and T_2 (circles) and two receivers R_1 and R_2 (squares).

Each transmitter transmits a signal in one channel defined in the $2.45\,\mathrm{GHz}$ IEEE 802.15.4 standard. The transmissions can occur simultaneously or with a small time offset in the range of a few μs caused by synchronization uncertainty and clock frequency offsets in the transmitters. The transmitted signals propagate to the receivers, where the time-difference-of-arrival $\Delta\tau_1$ and $\Delta\tau_2$ of the two incident signals is measured.

This leads to

$$\Delta\tau_1 = \tau_{21} - \tau_{11} + \tau_{to} = \quad \tau_0 + \tau_{to} \tag{1a}$$

$$\Delta\tau_2 = \tau_{22} - \tau_{12} + \tau_{to} = -\tau_0 + \tau_{to}, \tag{1b}$$

with an unknown time offset τ_{to} between the signal transmissions, and the quantity of interest τ_0 that is proportional to d_0. If the TDOA results (1a) and (1b) from both receivers are subtracted, the unknown transmission time offset is eliminated

$$\Delta\tau = \Delta\tau_1 - \Delta\tau_2 = \tau_{21} - \tau_{11} - \tau_{22} + \tau_{12} = 2\tau_0, \tag{2}$$

and the unknown distance between the transmitters can be calculated as

$$d_0 = c_0\tau_0 = \frac{c_0}{2}\Delta\tau, \tag{3}$$

where c_0 is the speed of light.

This derivation does not assume a specific way to measure $\Delta\tau_1$ and $\Delta\tau_2$. Our setup will use a combination of phase and time measurements to perform distance estimation.

B. Transmitter design

The transmitter shown in Fig. 2 consists of an IEEE 802.15.4 compatible radio chip, a micro controller and a chip antenna. The maximum output power is 0 dBm with an antenna gain of roughly 0 dBi. The transmitter is configured to transmit signals with channel switches in between.

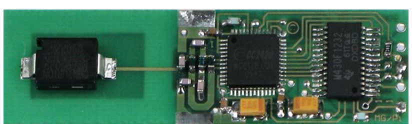

Fig. 2. Wireless transmitter unit. The dimensions are $53.5\,\mathrm{mm} \times 15.1\,\mathrm{mm}$. Note that the power supply (usually a battery) is not displayed.

C. Receiver design

The heterodyne receiver structure is shown in Fig. 3. With this design, the whole ISM band from 2400 to 2485 MHz is sampled with a sampling frequency of 250 MHz for development purposes. So, two or more channels can be received simultaneously. Future designs will consist of a dual-channel receiver with a considerably lower sampling rate.

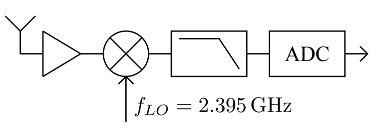

Fig. 3. Receiver design for distance measurement. The low pass filter bandwidth is 90 MHz and the sampling rate is $f_s = 250\,\mathrm{MHz}$.

For benchmark purposes, two synthesizers with different accuracy and stability are used as local oscillators (LO) during the measurements. Their characteristics can be found in Table I. The first synthesizer is equipped with a TCXO with very low phase noise (**A**), the second uses a low cost crystal oscillator (**B**). A comparison of the results from the two setups allows evaluation of the influence of frequency stability and phase noise of the receiver clocks on the measurement results.

TABLE I
PARAMETERS OF THE APPLIED LO SYNTHESIZERS

Setup	**A**	**B**
Reference oscillator	TCXO	XO
Frequency stability in ppm	2	50
Phase noise in dBc/Hz (offset 1 kHz)	−89	−76
Phase noise in dBc/Hz (offset 10 kHz)	−104	−91
Phase noise in dBc/Hz (offset 100 kHz)	−111	−83
Phase noise in dBc/Hz (offset 1 MHz)	−120	−113

III. SIGNAL PROCESSING

A prerequisite for precise distance measurement results under multipath conditions is the use of a large signal bandwidth [6]. A single channel in IEEE 802.15.4 offers only a bandwidth of approximately 2 MHz. However, the total available bandwidth in the ISM frequency band is 83.5 MHz. Key element of the proposed measurement method is the coherent combination of measurements from all 16 ZigBee channels, and the evaluation of signal phase. This allows for a significant accuracy enhancement compared to a single-channel measurement.

The first signal processing steps are the separation of the received signals in different channels, downconversion to complex baseband and sampling rate reduction. To calculate the time difference $\Delta\tau_{1/2}$ between the arrival of the signals from T_1 and T_2, the phase and time differences between the received signals and a reference signal held in receiver memory are computed. Both quantities contain the unknown propagation delay τ_0 and can be used for distance estimation. However, it is known from related techniques [7] that phase difference estimation yields considerably more accurate results than time difference estimation under typical conditions in wireless distance sensing. Our system therefore uses a combination of both quantities to allow precise distance measurements in a large unambiguous range.

Depending on the channel number n, the constant channel spacing f_d and the center frequency of the first channel f_0, the total measured phase difference $\Delta\varphi[n]$ can be expressed as

$$\begin{aligned}\Delta\varphi[n] &= \Delta\varphi_{21}[n] - \Delta\varphi_{11}[n] - \Delta\varphi_{22}[n] + \Delta\varphi_{12}[n] \\ &= 2\pi\frac{2d_0}{c_0}(f_0 + nf_d) + \varphi_0, \end{aligned} \tag{4}$$

where $\Delta\varphi_{ij}[n]$ denotes the evaluated phase difference between the signal from transmitter i received by receiver j and the reference signal. Any differences between transmitter and receiver phases are summarized into the unknown quantity φ_0, which must be constant over all channels and measurements to allow their coherent combination. This important demand can be met by ensuring a constant spacing between generated signal packets and the use of an appropriately designed channel sequence. Our setup was verified to comply with this reqirement by measurements.

For equidistant channel center frequencies (4) describes a linear function in n as shown in Fig. 4 (a). Its slope is propor-

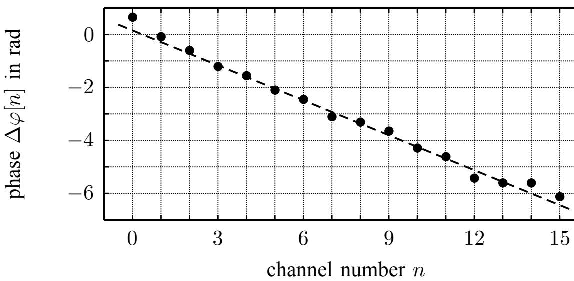

(a)

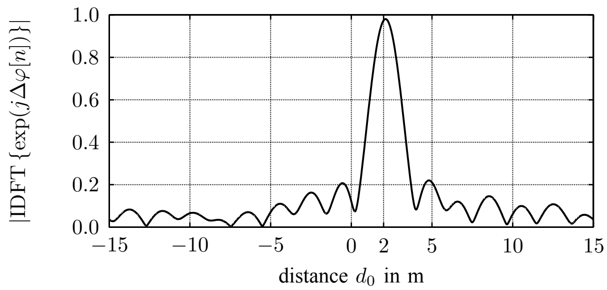

(b)

Fig. 4. (a) Phase ramp of a measurement sequence in 16 channels with a transmitter distance of $d_0 = 2\,\mathrm{m}$. Evaluated phase differences $\Delta\varphi[n]$ are marked with circles, the resulting estimated phase slope is indicated by a dashed line. (b) Corresponding zero-padded and normalized spectrum for slope estimation with a maximum peak close to the true distance d_0.

tional to the transmitter distance d_0, which can therefore either be estimated by a linear least-squares fit, or by applying an inverse discrete Fourier transformation (IDFT) to the complex phase ramp, allowing a spectrum-like analysis of the phase ramp pitch. The IDFT of a harmonic signal with phase $\Delta\varphi[n]$ evaluates to

$$\begin{aligned}\Delta\Phi[k] &= \mathrm{IDFT}\left\{\exp\left(j\Delta\varphi[n]\right)\right\}[k] \\ &= \Phi_0 \cdot \mathrm{IDFT}\left\{\exp\left(j\frac{4\pi n d_0 f_d}{c_0}\right)\right\}[k] \qquad (5)\end{aligned}$$

with

$$\Phi_0 = \exp\left(j\left(\frac{4\pi d_0 f_0}{c_0} + \varphi_0\right)\right). \qquad (6)$$

The constant phase term Φ_0 rotates the spectrum phase, but does not influence its magnitude, so that the phase ramp pitch is obtained as the position of the highest peak. An example for $N = 16$ channels and a transmitter distance of $d_0 = 2\,\mathrm{m}$ can be seen in Fig. 4 (b).

With the number of used channels N and the channel spacing f_d, the effective measurement bandwidth is $F = N f_d$, even if the actual $3\,\mathrm{dB}$ signal bandwidth is smaller than the channel spacing. This way, a much higher measurement accuracy can be realized than possible solely with time correlations. One disadvantage of this approach is the limitation of unambiguous distance estimation to

$$R = \pm\frac{c_0}{4 f_d}. \qquad (7)$$

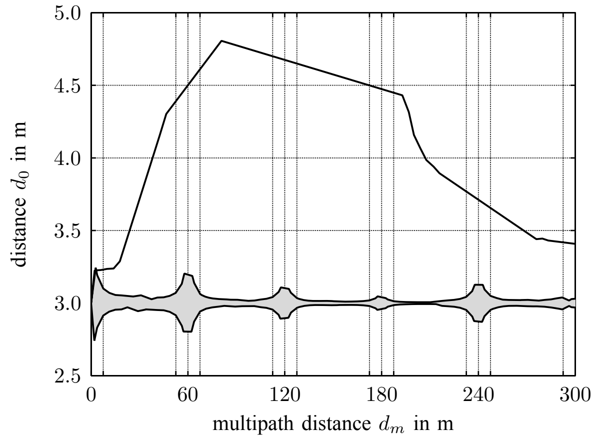

Fig. 5. Simulated distance d_0 over additional multipath distance d_m between T_2 and R_1. The expected distance is $d_{0,exp} = 3\,\mathrm{m}$. Filled envelope shows the estimation using phase measurements, the line indicates averaged results from time measurements. The additional unlabeled grid lines are $7.5\,\mathrm{m}$ apart from the labeled lines.

Range limitation can be avoided by using time difference estimation that is unambiguous in the entire evaluation range. As the time difference estimation process is heavily affected by multipath and shadowing effects, the average over all N channels is used. If d_{0a} and d_{0t} are the results from phase and time difference evaluation, respectively, the unambiguous distance d_0 can be expressed as

$$d_0 = d_{0a} + n\frac{c_0}{2 f_d} \qquad (8)$$

with

$$n = \arg\min_{k\in\mathbb{Z}} \left| \left(d_{0a} + k\frac{c_0}{2 f_d} \right) - d_{0t} \right|. \qquad (9)$$

This approach yields correct results as long as the error expected from time difference measurements is smaller than the unambiguity range R, thus imposing a lower limit on the number of channels to be used.

IV. Application

In our demonstrator the parameters $N = 16$ channels with a spacing of $f_d = 5\,\mathrm{MHz}$ are used, which leads to an effective bandwidth of $F = 80\,\mathrm{MHz}$. The unambiguity range is $R = \pm 15\,\mathrm{m}$, which we suppose to be larger than the error expected from time difference measurements. The actually occupied bandwidth is approximately $N \cdot 2\,\mathrm{MHz} = 32\,\mathrm{MHz}$. For reducing the required computational effort only the first $32\,\mu\mathrm{s}$ of the measured signals are used for evaluation, which correspond to 256 samples at a sampling rate of $8\,\mathrm{MHz}$ after downconversion to complex baseband.

A. Simulation results

The DSSS (Direct Sequence Spread Spectrum) code of the PHY layer in IEEE 802.15.4 has a chip rate of $f_c = 2\,\mathrm{MHz}$. This allows for complete multipath seperation by time correlations, if there is an additional travelling distance of $\frac{2c_0}{f_c} = 300\,\mathrm{m}$. The phase evaluation algorithm on the other

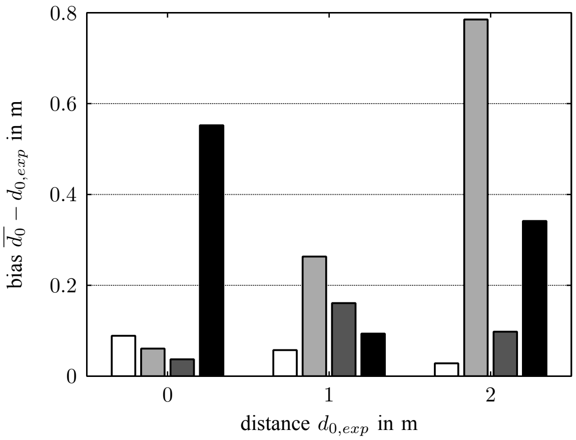

Fig. 6. Differences from measured to expected distances for phase (white, dark gray) and time (light gray, black) related measurements. White and light gray shading indicates the use of TCXO clocks (A), and dark gray and black shading marks the use of XO clocks (B) in both receivers.

hand can distinguish two paths in the spectrum, as soon as they are $\frac{2c_0}{Nf_d} = 7.5\,\mathrm{m}$ apart [6]. In order to demonstrate the improved multipath behavior of our system, a simulation with the system parameters mentioned above was created. The direct paths remain unchanged, while a multipath is added to the communication link between T_2 and R_1 with constant power ratio of $10\,\mathrm{dB}$. The additional multipath travelling distance is increased from 0 to $300\,\mathrm{m}$. Fig. 5 approves the multipath behavior derived above.

B. Measurement results

In our setup, the receivers were placed $11.4\,\mathrm{m}$ apart, and at least 100 measurements were made for each transmitter distance of $d_{0,exp} = 0, 1, 2\,\mathrm{m}$.

The results are analyzed regarding average measurement error (bias) and standard deviation. Fig. 6 shows the biases measured with different distances and receiver clocks. For distance estimations from phase measurements, the biases reside below $16\,\mathrm{cm}$ for XO and below $9\,\mathrm{cm}$ for TCXO clocked receivers. Time measurements lead to larger biases of up to $79\,\mathrm{cm}$. Here, no clear improvement of TCXO clocked receivers can be seen.

The error histograms in Fig. 7 illustrate the impact of the receiver clock stability on the measurement standard deviation that is indicated by vertical dashed lines. Values for the histograms are averaged over all three measurement positions, because the standard deviations did not significantly change with varying distances. With phase estimations, the standard deviation is lower by a factor of 7.7 for TCXO, and by factor of 13 for XO clocked receivers. The improvement over time estimations is therefore slightly lower than the number of channels used, which can be explained by the averaging of time estimations, which generates an enhancement as well. With the low cost crystal oscillator (XO) the standard deviation is by factors 7.1 (phase estimations) and 4.1 (time estimations) higher than observed with TCXO clocked receivers.

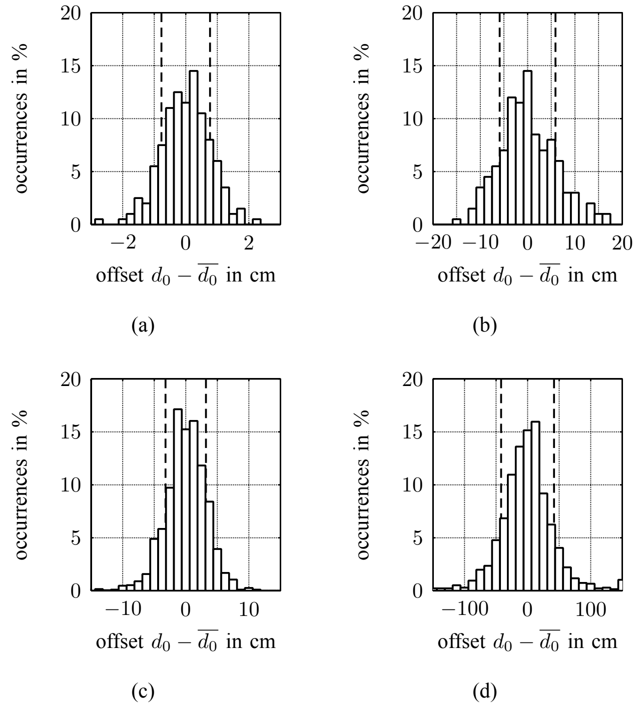

Fig. 7. Unbiased histograms of measurement errors. The ordinates show the number of occurences. a) TCXO/phase. b) TCXO/time. c) XO/phase. d) XO/time.

V. Conclusion

In this work we have demonstrated the use of usual IEEE 802.15.4 (ZigBee) communications transceivers for highly accurate position estimation. Due to the coherent synthesis of a sequence of measurements from all available frequency channels it is possible to mitigate perturbations from multipath propagation effectively. The presented techniques can easily be adapted to many other communications standards, and it is favorable where low-cost and precise localization of commercial communications transponders is desired.

References

[1] E. Mackensen, W. Kuntz and C. Muller, "Smart wireless autonomous microsystems (SWAMs) for sensor actuator networks," *IEEE Sensors for Industry*, pp. 72–78, Jan. 2004.

[2] P. Havinga, B. Dil and M. Bijl, "Localization schemes integration with ZigBee communication protocol stack," *1st European ZigBee Developers' Conference*, June 2007.

[3] S. Lanzisera, D. Lin and K. Pister, "RF Time of Flight Ranging for Wireless Sensor Network Localization," *Fourth Workshop on Intelligent Solutions in Embedded Systems*, p. 12pp, June 2006.

[4] A. Stelzer, K. Pourvoyeur and A. Fischer, "Context and application of LPM—A novel 3-D local position measurement system," *IEEE Trans. Microwave Theory Tech.*, vol. 52, no. 12, pp. 2664–2669, Dec. 2004.

[5] M. Vossiek, L. Wiebking, P. Gulden, J. Wieghardt, C. Hoffmann and P. Heide, "Wireless local positioning," *IEEE Microwave Magazine*, vol. 4, no. 4, pp. 77–86, Dec. 2003.

[6] J. Scheer and J. Kurtz, *Coherent Radar Performance Estimation*, Artech House Inc., 1993.

[7] E. Kaplan and C. Hegarty, *Understanding GPS*, Artech House Inc., 2nd ed., 2006.